



Synthesis, docking, and biological evaluation of thiazolidinone derivatives against hepatitis C virus genotype 4a

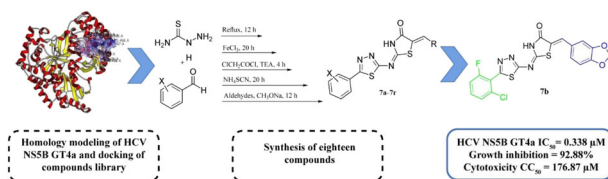
Ahmed S. Al-Behery¹ · Kamel M. Elberembally¹ · Mohammed A. Eldawy¹

Received: 23 December 2020 / Accepted: 15 March 2021 / Published online: 26 March 2021
© The Author(s), under exclusive licence to Springer Science+Business Media, LLC, part of Springer Nature 2021

Abstract

Hepatitis C virus (HCV) genotype 4a (GT4a) is prevalent in Egypt. It did not gain the necessary scientific focus despite its high resistance. Since the crystal structure NS5B (RNA-dependent RNA polymerase) of HCV GT4a has not been resolved until now, homology modeling was conducted to build and validate the 3D model of the enzyme. Ligand binding sites including the allosteric thumb II pocket were detected and used in lead optimization. Sixty new 4-thiazolidinone derivatives have been virtually designed and docked into thumb II site of HCV NS5B GT4a using rigid docking approach. Eighteen compounds (**7a–r**) that show good docking scores were synthesized and tested in vitro against NS5B GT4a. Compounds **7b** and **7n** showed the best inhibitory activity ($IC_{50} = 0.338$ and $0.342 \mu\text{M}$, respectively). Compounds **7a**, **7b**, **7c**, **7d**, **7k**, **7n**, **7q**, and **7r** that have IC_{50} values less than $2 \mu\text{M}$ were assessed for cellular anti-HCV GT4a activity using human hepatoma cell line (Huh 7.5). The percentages of viral growth inhibition are between 79.67 and 94.77%. Compound **7b** is the most active in the in vitro and cellular assays and could be considered a potential new lead for future anti-HCV studies.

Graphical Abstract



Keywords HCV NS5B GT4a · Thiazolidinones · Homology modeling · Molecular docking

Introduction

Hepatitis C virus (HCV) infection is considered as an immense burden on global health because it is the leading cause of liver cancer. Globally, an estimated 71 million people are infected with chronic HCV and susceptible to develop liver cirrhosis

and hepatocellular carcinoma [1]. The high cost of treatment is the major challenge for HCV-infected patients in developing countries. In Egypt, where HCV genotype 4a (GT4a) infection hits 30% of the population and represents 15% of the global HCV infections, the treatment of HCV has become a national health concern [2]. Boceprevir, Telaprevir, Simeprevir, Ombitasvir, Sofosbuvir, and Dasabuvir are directly acting antivirals (DAA), which have been used in the form of combination therapies for HCV treatment [3–5]. HCV therapy has been progressed rapidly with particular focus on GT1a and GT1b, while the battle against GT4a requires more efforts because of the high resistance, progressive mutations, and pharmacoeconomic aspects [6, 7].

HCV NS5B is the responsible enzyme for genome replication of the HCV [8]. DAA drugs can manipulate the polymerase function of viruses either through the active

Supplementary information The online version contains supplementary material available at <https://doi.org/10.1007/s00044-021-02721-w>.

✉ Ahmed S. Al-Behery
ahmed.samir.chem@pharm.tanta.edu.eg

¹ Faculty of Pharmacy, Tanta University, El Geish Street, Tanta 31527, Egypt

(orthosteric) site by providing false nucleotide substrates leading to RNA chain termination or through the allosteric sites to inhibit RNA synthesis [8]. The NS5B structure features a classical “right hand” architecture of the polymerase family, which is characterized by the GDD functional motif (Gly317-Asp318-Asp319), which contains the orthosteric site. The fingers, palm, and thumb domains hold the allosteric sites (Fig. 1) [8, 9].

Non-nucleoside inhibitors are a class of small molecules that target the NS5B allosteric sites that are thumb I, thumb II, palm I, palm II, and palm III [8]. The binding of inhibitors to these sites results in a conformational change of the active site. Thumb II site is shallow and hydrophobic pocket at the base of the thumb domain. It is 35 Å away from the orthosteric site [10].

Thumb II inhibitors (Fig. 2) include dihydropyrene [11], thiophene carboxylic acid [12], and 2-arylimino-4-thiazolidinone [13] scaffolds (pink color). These scaffolds

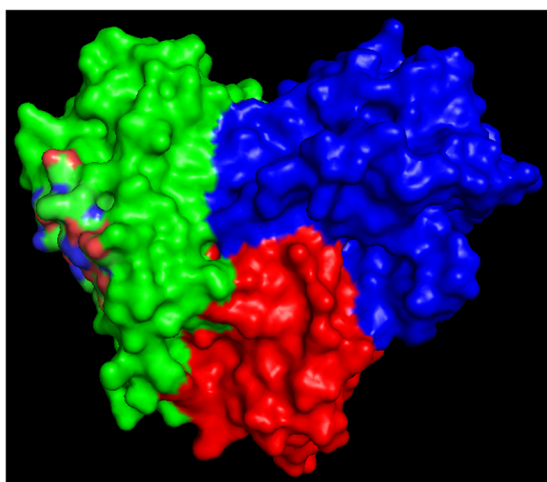


Fig. 1 HCV NS5B crystal structure (PDB: 3FRZ) showing palm (red), thumb (blue), and finger (green) domain. The image generated by PyMOL4.0.4 [43]

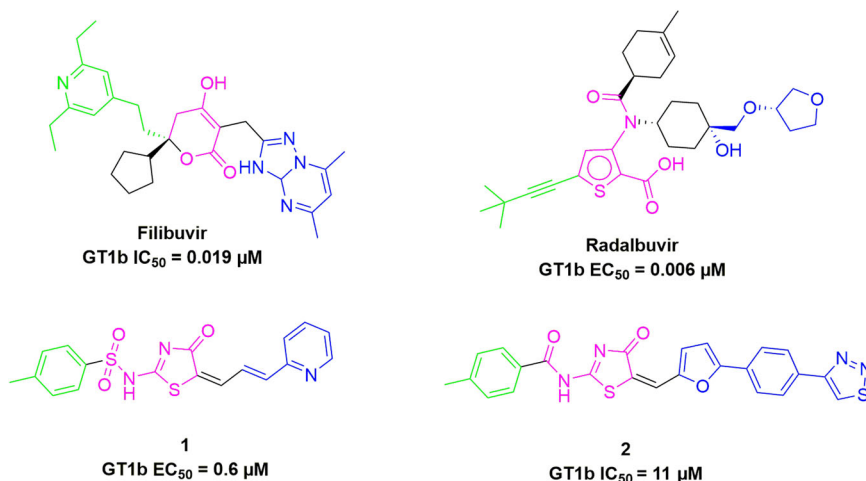
engage the thumb II site by hydrogen bonding with the backbone NH of Ser476 and Tyr477 and the side chain of Arg501. While right side substituents (blue color) provide hydrogen bond donor and acceptor atoms, the left side substituents (green color) offer hydrophobic contacts with the lipophilic amino acids of the pocket [14, 15].

Filibuvir, with a dihydropyrene scaffold, is a potent and selective inhibitor with IC_{50} of 0.019 μM against GT1b [16]. The triazolopyrimidine ring forms a π - π stacking interaction with His475; this ring is linked to the dihydropyrene core by a methylene group. Hydrophobic interaction between the thumb II site and one of the ethyl groups of the pyridine has provided good enzymatic potency [14]. Phase II clinical candidate Radalbuvir (GT1b EC_{50} = 0.006 μM) discovery led by the introduction of heterocyclic ethers on the N-alkyl substituent hydroxyl groups. The heterocyclic ether modulates protein binding and enhances the pharmacokinetic profile [15].

Both compounds **1** (GT1b EC_{50} = 0.6 μM) [17] and **2** (GT1b IC_{50} = 11 μM) [17] have similar hydrophobic substituents (green color), while they differ in the right side substituents. Compound **1** has extended pyridine-2-yl and compound **2** contains 1,2,3-thiadiazole to provide hydrogen bond acceptor atoms. Thiazolidinones were reported to have versatile biological activities including antiproliferative, antibacterial, antifungal [18–20]. Cyclooxygenase enzymes can be targeted by these compounds, which make thiazolidinones good scaffold to develop anti-tumor and anti-inflammatory agents [21]. Furthermore, thiazolidinone compounds have been shown to inhibit the HIV-1 reverse transcriptase [22].

Recently, it has been reported that coupling of the 1,3,4-thiadiazole ring with 4-thiazolidinone resulted in leads that strongly inhibit HCV GT1b NS5B [23, 24]. These studies have indicated that bioactivity was improved by increasing the lipophilicity of the scaffold. Also studies indicated that

Fig. 2 HCV NS5B thumb II inhibitors



condensation of arylidene moiety on 1,3-thiazolidine-4-one ring could be essential for anti-HCV NS5B activity [23, 24]. However, this scaffold has not been tested yet for the resistant GT4a. In this study, the HCV GT4a NS5B model showed a polar region composed of Arg501, Arg505, Arg498, Lys531, and Lys533 that can be targeted by compounds with hydrogen bond acceptor functional groups. Compounds **7b**, **c**, **f**, **g**, **j**, **l**, **m**, **n**, **q**, and **r** were synthesized and biologically evaluated to test this hypothesis. Furthermore, compound **7e** with an extended alkyl side chain was synthesized and explored for better fitting in the lipophilic pocket. Compound **7a** (Fig. 3) was reported to have good activity on HCV NS5B GT1b ($IC_{50} = 25.3 \mu\text{M}$) [23] and it is used in this study as a lead for the design of the new compounds.

Accordingly, a set of compounds with diverse substitutions on ring A and B (Fig. 3) has been designed, taking into consideration the features of the thumb II GT4a binding site and previous reports. Ring A (green color) should have halogens, while ring B (blue color) could be derivatized with halogens, hydrogen bond donor/acceptor functional groups, or extended alkyl side chains. A homology model of HCV NS5B GT4a was constructed and the compounds were docked into thumb II binding site in order to validate the binding affinity of the designed set of compounds. Based on the docking results, 18 compounds were selected for synthesis and were further evaluated for their activity.

Results and discussion

Homology modeling

The sequence of HCV NS5B GT4a was obtained from the UniProt database [25]. SWISS-MODEL server has been used to build the homology model (Supplementary Fig. S46, Supplementary Material).

A BLAST search of HCV NS5B GT4a against PDB sequence entries shows a match with 77.54 sequence identity. The SWISS-MODEL server was used to generate homology model for HCV NS5B GT4a. Global Model Quality Estimation (GMQE) and Qualitative Model Energy Analysis (QMEAN) scoring functions were used as an initial criterion to discriminate good from bad models. The model shows -0.09 QMEAN score (Supplementary Fig. S45a, Supplementary Material), which indicates good agreement between the homology model and experimental structures of the same size. The local quality estimate plot (Supplementary Fig. S45b, Supplementary Material) shows that there are no residues that gave a score below 0.6, which indicates high model quality. In the comparison plot (Supplementary Fig. S45c, Supplementary Material), the homology model is shown as a red star, and it is aligned with QMEAN score within one standard deviation of the mean $|Z$ -score as the experimental structures represented in black dots.

After building the homology model, it was subjected to protein refinement using the ModRefiner server [26]. Validation was carried out to explore the stereochemical quality of dihedral angles Φ against Ψ of amino acid residues in the homology model and identify sterically allowed regions for these angles. Validation was carried out using SWISS-MODEL structure assessment online server [27] (Fig. 4). The Ramachandran plot of modeled HCV NS5B protein (Fig. 4A) shows 0.75 MolProbity score, 98.04% Ramachandran favored, and 0.18% Ramachandran outliers. The glycine and proline Ramachandran plot (Fig. 4B, C) show no outliers in disallowed regions.

Molecular docking

The docking procedure was validated by using crystal structure of HCV NS5B GT1b in complex with Filibuvir (PDB: 3FRZ) [14]. The redocked binding pose of Filibuvir in GT1b observed overlays the original crystal structure

Fig. 3 The designed set of compounds with diverse substitutions on rings A and B

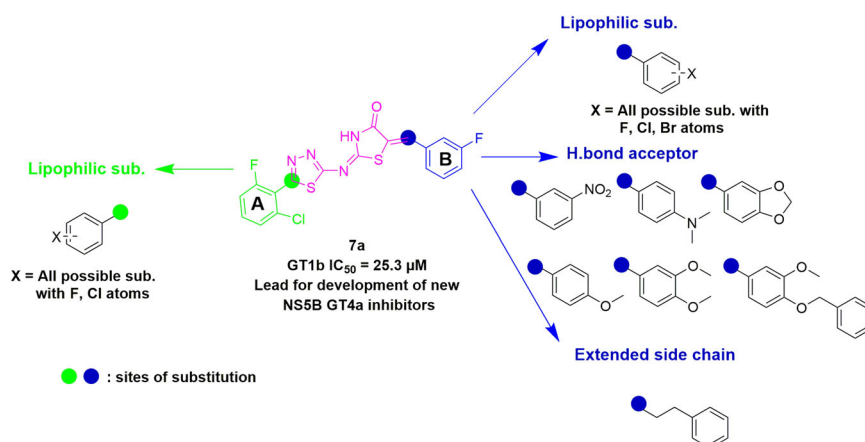


Fig. 4 The Ramachandran plot of modeled HCV NS5B protein using SWISS-MODEL structure assessment online server,

A General Ramachandran plot, **B** Glycine Ramachandran plot, **C** Proline Ramachandran plot. Favored regions are shown in green, additional allowed region shown in light green, generously allowed regions are shown in pale green, and disallowed regions shown in white

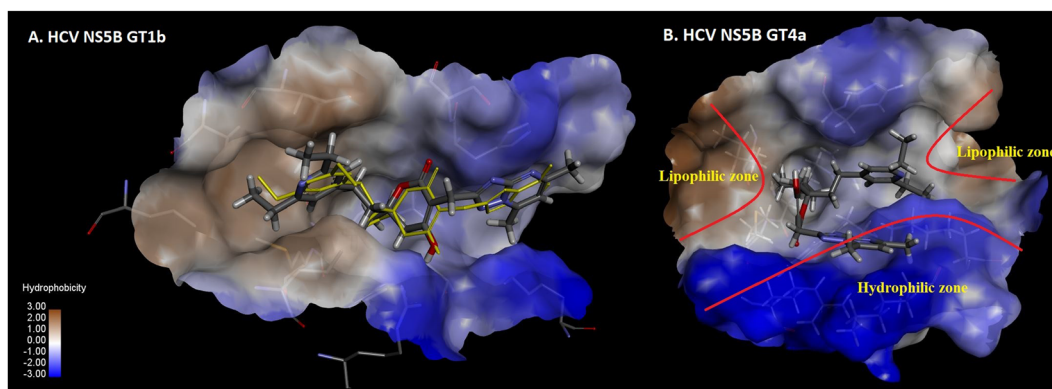
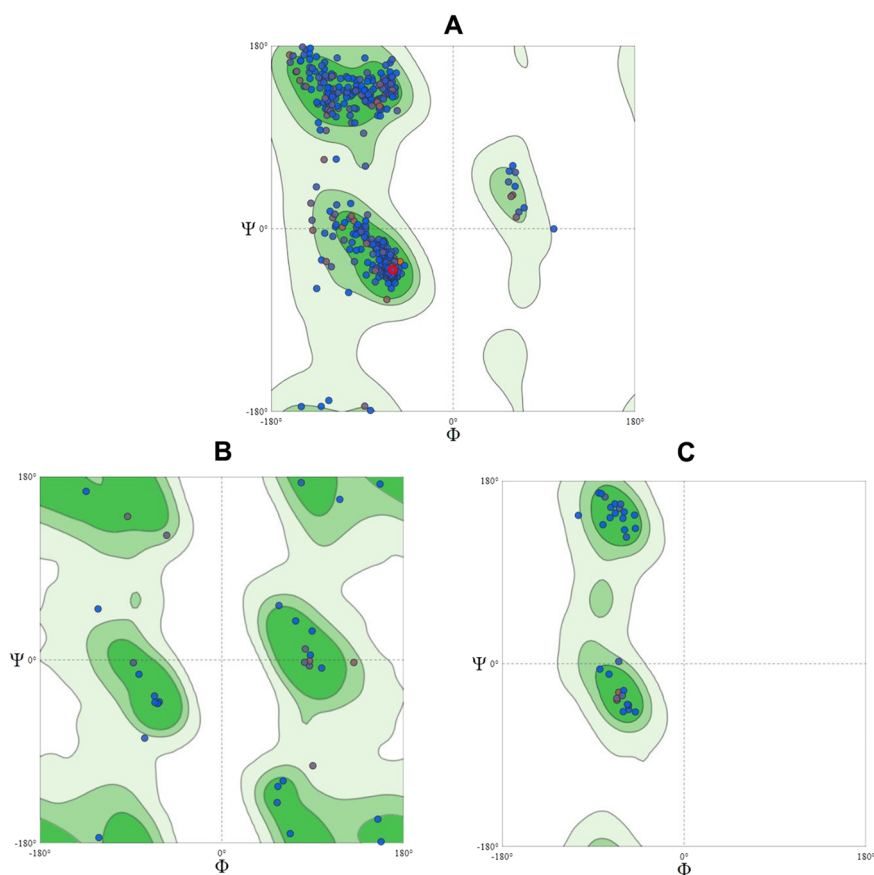


Fig. 5 **A** Docking pose of Filibuvir to HCV NS5B GT1b thumb II site overlaying on the original crystal structure binding pose. **B** Docking pose of Filibuvir to HCV NS5B GT4a thumb II site and showing the new features of the allosteric pocket in GT4a

binding pose with the same binding interactions as reported (Fig. 5A). The same established grid box coordinates in HCV NS5B GT1b was taken as a model to expect the binding site of HCV NS5B GT4a.

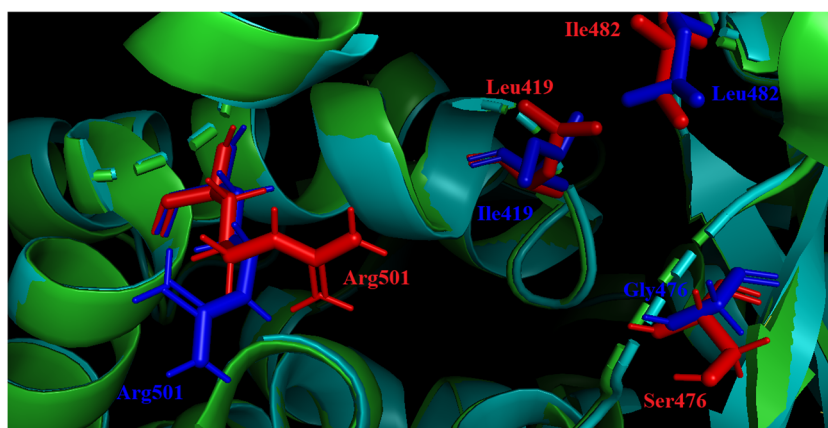
The docking score of Filibuvir was decreased from -12.78 against HCV NS5B GT1b to -8.84 against HCV NS5B GT4a. This decline indicates that the features of the binding site in the HCV NS5B GT4a model changed (Fig. 5B). Two lipophilic surfaces were detected in thumb II GT4a, one of them was similar to GT1b. Hydrophilic

surface, also, was detected in thumb II GT4a that can be targeted for hydrogen bonding and electrostatic interactions by the studied compounds (Fig. 5B).

The alignment of the 3D structure of GT1b crystal structure and the GT4a homology model was carried out to analyze the differences in the amino acids and the spatial arrangement of the critical residues of interaction (Fig. 6).

HCV NS5B GT1b thumb II site consists of Leu497, Leu419, Ile482, Val376, His475, Trp528, Ser476, and Arg501. These amino acids are the key amino acids for

Fig. 6 Alignment of the 3D structure of HCV NS5B GT1b crystal structure (green color) (PDB: 3FRZ) and HCV NS5B GT4a homology model (cyan color). Ser476, Leu419, Ile482, and Arg501 (red color) are of HCV NS5B GT1b, Gly476, Ile419, Leu482, and Arg501 amino acids (blue color) are of HCV NS5B GT4a. The image was generated by PyMOL4.0.4 [43]



interaction with the reported active compounds of dihydropyrene, thiophene carboxylic acid, and 2-arylimino-4-thiazolidinone scaffolds [28]. However, in HCV NS5B GT4a thumb II there are three amino acid mutations reported, **S476G**, **I482L**, and **L419I** that render the binding site more lipophilic and confer a high level of resistance [6, 7]. These findings indicate that the binding site of HCV NS5B GT4a lost the features of interactions that afforded in HCV NS5B GT1b. Thus, the designed compounds should have functional groups that afford more hydrogen bond interactions with optimal lipophilicity. Also, compounds with extended side chains will be investigated for a suitable fitting of the molecule to the binding site.

Docking results showed that the thiadiazole ring with substituted halogenated phenyl derivatives interacts with the hydrophobic region of thumb II site, which indicates that these compounds can be active against HCV NS5B GT4a. The top 18 compounds were selected for synthesis and biological evaluation (Table 1).

Chemistry

Compounds **7a–r** were synthesized according to Scheme 1. Thiosemicarbazide **2** and different aldehydes **1a–e** reacted with each other to give the thiosemicarbazone derivatives **3a–e**.

Compounds **3a–e** undergo oxidative cyclization into 2-Amino-1,3,4-thiadiazole derivatives **4a–e** [23]. A suggested mechanism for the oxidative cyclization is shown in Scheme 2 [23, 29]. According to this mechanism, reaction is initiated by deprotonation, forming a radical at thiosemicarbazone N2. The resonance hybrid thiol radical attacks azomethine carbon to form the ring. The expulsion of another hydrogen radical finally yields 5-aryl-1,3,4-thiadiazole-2-amines [23, 29].

Compounds **4a–e** were converted to compounds **5a–e** by reaction with chloroacetyl chloride in the presence of trimethylamine. The synthesis of compounds **6a–e** was carried out by the reaction of compounds **5a–e** with ammonium

thiocyanate [23]. Compounds **5a–e** react with ammonium thiocyanate to form intermediates that undergo intramolecular cyclization to generate compounds **6a–e** as indicated in Scheme 3 [30].

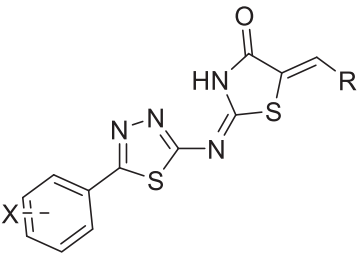
The target compounds **7a–r** were obtained by the reaction of compounds **6a–e** with different aldehydes in the presence of sodium methoxide [23].

Compounds **3a–e**, **4a–e**, **5a–e**, and **6a–e** were previously reported [23, 24], while compounds **7a–r** are new and confirmed through elemental and spectroscopic analysis. Elemental analysis (within the accepted limits ($\pm 0.4\%$)) confirms the purity of the final compounds and the spectroscopic data of the synthesized final compounds **7a–r** agreed with the expected chemical structures as given in the experimental section.

IR of compounds **7a–r** shows one broad peak in the range ($3450\text{--}3300\text{ cm}^{-1}$) of the lactam NH and peak at 1720 cm^{-1} of the carbonyl functional group in the thiazolidinone ring. ^1H NMR shows the characteristic singlet at (12.5–13.5 ppm) that is assigned to NH of 1,3-thiazolidin-4-one ring and the peaks of the aromatic protons and exocyclic =CH- proton were found in the range of (7–8 ppm). The ^1H NMR spectra of the compounds **6a–e** were characterized by the (singlet, 2H) peak of the active methylene in 1,3-thiazolidin-4-one ring at 4.1 ppm [23]. The absence of this peak in ^1H NMR of compounds **7a–r** confirms the condensation of the different aldehydes and formation of the target final compounds (**7a–r**). The exocyclic =CH- proton in compounds **7a–r** showed singlet peak with resonances at 7.70–8.10 ppm within the aromatic peaks range of 7–8 ppm. 5-Arylidene-1,3-thiazolidinones exist as *Z* configurational isomer as evidenced by previous literature reports of the ^1H NMR [31] and X-ray crystallography [32].

The ^{13}C NMR spectra of the reported compounds **6a–e** characterized by the thiazolidinone C5 signal at the range of (30–38 ppm) [23], while the corresponding carbon signals in the final compounds **7b–f**, **7n**, and **7q** were shifted to the range of (135–155 ppm).

^1H - ^1H correlation spectroscopy (COSY) and heteronuclear single quantum correlation (HSQC) experiments were carried

Table 1 The docking scores and IC₅₀ results of the synthesized compounds (**7a–r**)


Compound	X	R	Chemgauss4 scores (HCV NS5B GT4a)	IC ₅₀ ^a ± SD ^b (μM) (HCV NS5B GT4a)
7a	2-Chloro-6-fluoro	3-Fluorophenyl	-9.70	1.029 ± 0.02
7b	2-Chloro-6-fluoro	1,3-benzodioxol-5-yl	-9.82	0.338 ± 0.01
7c	2-Chloro-6-fluoro	4-Dimethylaminophenyl	-9.9	0.634 ± 0.01
7d	2-Chloro-6-fluoro	3-Chlorophenyl	-9.74	1.882 ± 0.04
7e	4-Fluoro	Phenylethyl	-10.28	5.006 ± 0.11
7f	4-Fluoro	3,4-Dimethoxyphenyl	-9.14	4.128 ± 0.09
7g	4-Chloro	4-(benzyloxy)-3-methoxyphenyl	-9.92	11.760 ± 0.26
7h	3-Fluoro	3-Bromophenyl	-9.97	2.401 ± 0.05
7i	3-Fluoro	2-Bromophenyl	-10.19	6.660 ± 0.15
7j	3-Fluoro	4-Dimethylaminophenyl	-10.11	5.770 ± 0.13
7k	3-Fluoro	3-Chlorophenyl	-9.86	0.564 ± 0.01
7l	3-Fluoro	4-Methoxyphenyl	-9.8	2.670 ± 0.06
7m	2-Chloro	4-(benzyloxy)-3-methoxyphenyl	-10.06	8.565 ± 0.19
7n	2-Chloro	4-Dimethylaminophenyl	-10.23	0.342 ± 0.01
7o	2-Chloro	3-Bromophenyl	-10.22	2.193 ± 0.05
7p	2-Chloro	3-Chlorophenyl	-10.2	2.954 ± 0.06
7q	2-Chloro	3-Nitrophenyl	-10.02	0.642 ± 0.01
7r	2-Chloro	4-Methoxyphenyl	-10.09	0.936 ± 0.02

^aThe half-maximal inhibitory concentration^bThe standard deviation of triplicate experiments

out for compound **7b** as a representative example for further structural confirmation. The atom numbering of compound **7b** was generated by ChemBioDraw software [33] specifically for NMR analysis. The ¹H-¹H COSY (Supplementary Fig. S5, Supplementary Material) confirms the ¹H NMR assignment as follow; signal at 7.2 ppm (H21) is correlated with signal at 7.3 ppm (H22), signal at 7.7 ppm (H18) is correlated with signals at 7.5 ppm (H17) and 7.6 ppm (H19). HSQC (Supplementary Fig. S6, Supplementary Material) spectrum indicates that the exocyclic H13 singlet signal at 7.8 ppm in ¹H NMR is correlated with 134.83 ppm (C13) in ¹³C NMR that is more de-shielded than C21, C22, and C25, while the signal at 126.18 ppm (C25) is correlated with 7.3 ppm (H25) that

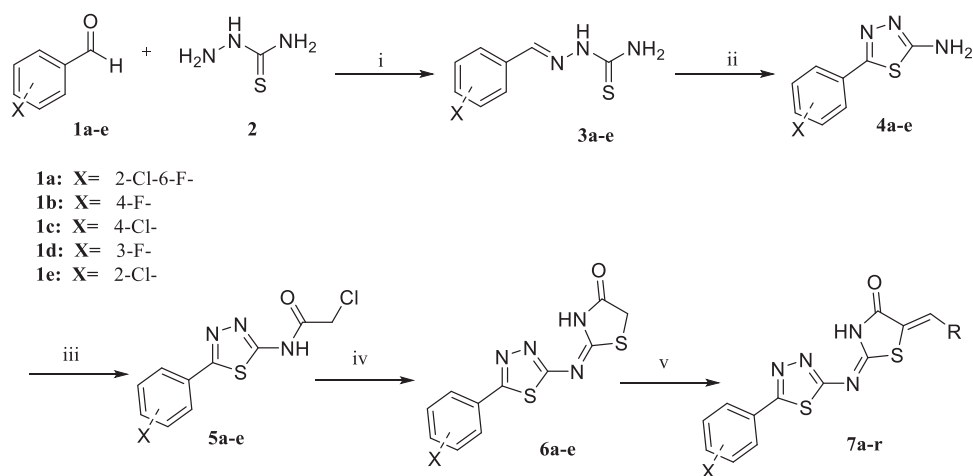
confirms the assignment of the signal at 7.3 ppm to H22. Signal at 115.07 ppm (C17) is correlated with 7.5 ppm (H17), signal at 126.21 ppm (C19) is correlated with 7.6 ppm (H19), and signal at 135.86 ppm (C18) is correlated with 7.7 ppm (H18).

Biological evaluation and molecular modeling studies

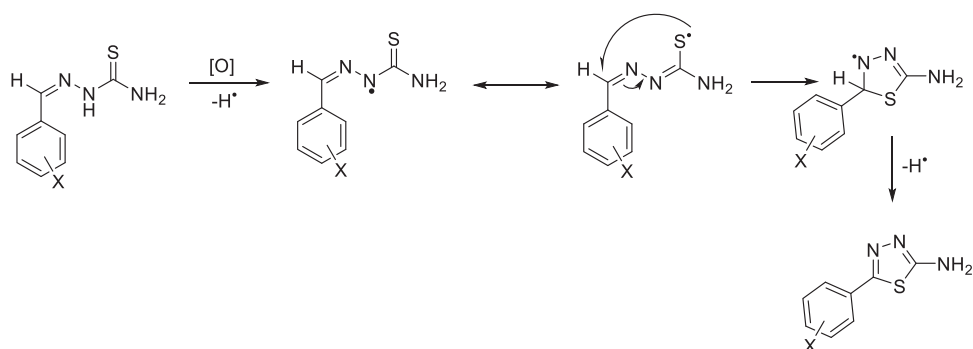
In vitro HCV NS5B GT4a inhibition assay

The HCV NS5B GT4a inhibition assay is carried out on 18 synthesized compounds **7a–r** (Table 1). The results show that compound **7a** (IC₅₀ = 1.029 μM) is 25 folds more

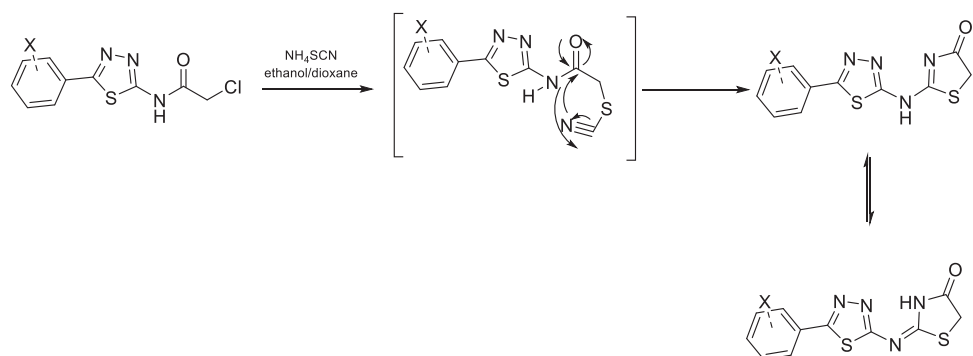
Scheme 1 Synthetic route for compounds **7a–r**. (i) Acetic acid, reflux, 12 h; (ii) Ferric chloride, ethanol, reflux, 20 h; (iii) Chloroacetyl chloride, triethylamine, dichloromethane, 4 h; (iv) Ammonium thiocyanate, reflux, 20 h; (v) Different aldehydes, CH_3ONa , methanol, reflux, 12 h



Scheme 2 The mechanism of 1,3,4-thiadiazole ring formation



Scheme 3 The mechanism of thiazolidin-4-one ring formation



potent on HCV NS5B GT4a than reported on HCV NS5B GT1b ($\text{IC}_{50} = 25.3 \mu\text{M}$) [23], from which we conclude that 2-[(5-substituted phenyl)-1,3,4-thiadiazol-2-yl]imino]-5 (substituted phenylmethylidene)-1,3-thiazolidin-4-one scaffold is more potent on HCV NS5B GT4a.

The NS5B inhibitory assay results illustrate that compounds **7a–d** and **7n–r** having 2-Chloro-6-fluorophenyl and 2-Chlorophenyl ring A substitution on ring A respectively exhibit better HCV NS5B inhibition activity than 3-Fluoro, 4-Fluoro, and 4-chloro substitutions. Among the series **7a–d** and **7n–r**, compounds **7b** and **7n** ($\text{IC}_{50} = 0.338$ and $0.342 \mu\text{M}$, respectively) are the most potent compounds.

Compound **7b** is considered to be three folds more potent than the lead compound **7a** ($\text{IC}_{50} = 1.029 \mu\text{M}$ on HCV NS5B GT4a). Also, compound **7b** is considered to be 74 folds more potent than the lead compound **7a** ($\text{IC}_{50} = 25.3 \mu\text{M}$ on HCV NS5B GT1b).

Analysis of the results focusing on ring B and considering compounds **7a–d**, **7h**, **7k**, **7l**, **7n–r** reveals that the substitution on meta or para positions is more favorable than substitution on ortho position, as exhibited by the IC_{50} values of compounds **7h** and **7i** showing IC_{50} 2.401 and $6.66 \mu\text{M}$, respectively. The results show that the most active four compounds are **7b**, **7c**, **7k**, **7n**, which can be explained

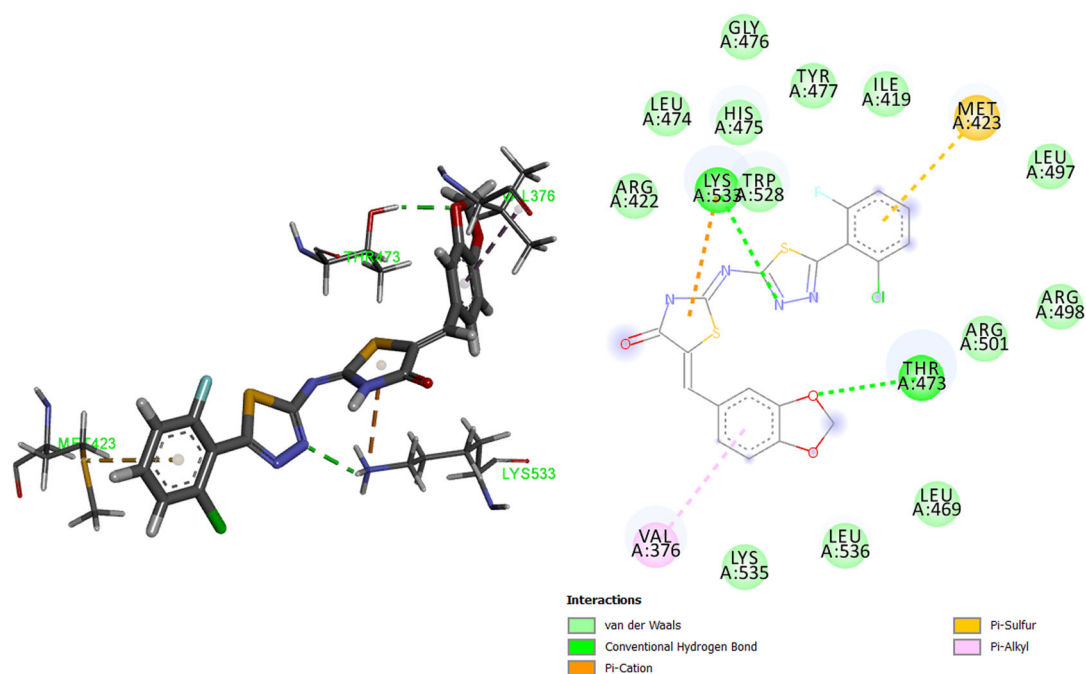


Fig. 7 The 3D (left) and 2D (right) of the docking interactions of compound **7b** with HCV NS5B GT4a thumb II site

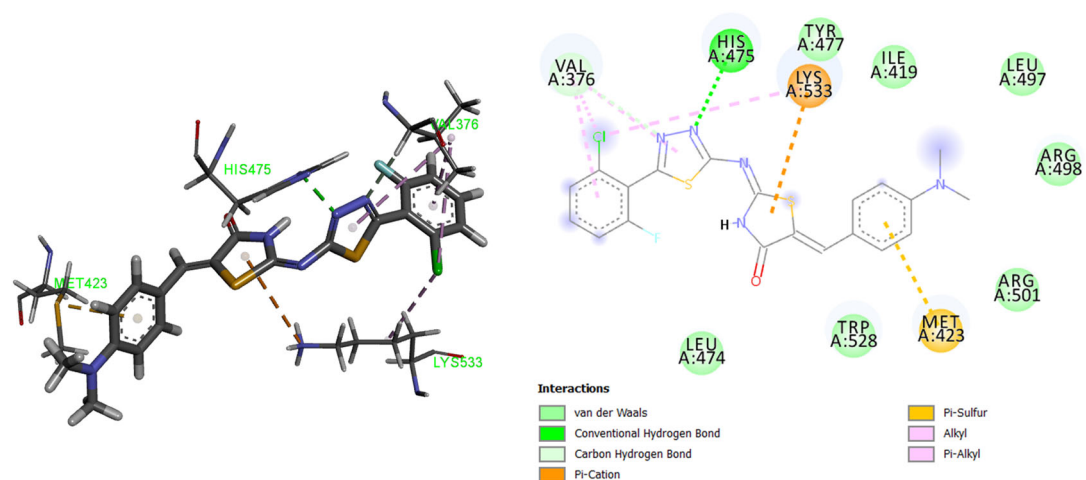


Fig. 8 The 3D (left) and 2D (right) of the docking interactions of compound **7c** with HCV NS5B GT4a thumb II site

by the docking studies. Generally, the most prominent interaction type of compounds **7a–r** (Figs. 7–10, and S47–S60, Supplementary Material) with the surrounding amino acids is in the form of hydrogen bonding through the carbonyl oxygen and the NH group of the thiazolidinone ring. Analysis of the binding interactions of **7b**, **7c**, **7k**, and **7n** with the thumb II site is summarized in Table 2.

The most active compound **7b** forms two hydrogen bonds with Lys533 and Thr473, and it shows hydrophobic contacts with many hydrophobic amino acids in the binding site (Fig. 7 and Table 2).

The decrease in the biological activity of compound **7c** could be explained by the inability to form two hydrogen bonds compared to compound **7b**. Compound **7c** forms one hydrogen bond with His475 amino acid. Also, it has fewer nearby hydrophobic interactions (Fig. 8 and Table 2).

Compound **7k** forms three hydrogen bonds with His475, Arg422, Thr473 amino acids, and shows less hydrophobic interactions through aromatic rings. Also, hydrogen bond distance with Arg422 is less than optimum (Fig. 9 and Table 2).

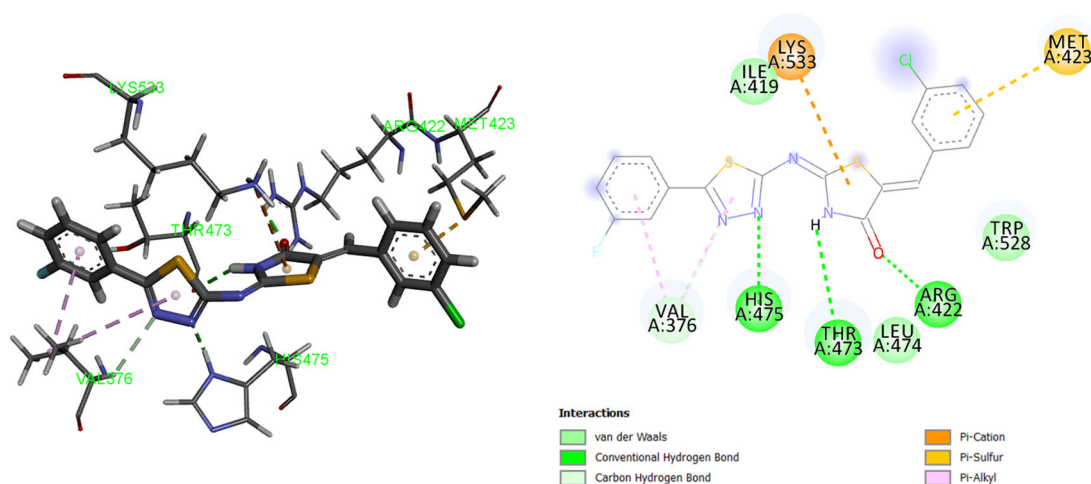


Fig. 9 The 3D (left) and 2D (right) of the docking interactions of compound **7k** with HCV NS5B GT4a thumb II site

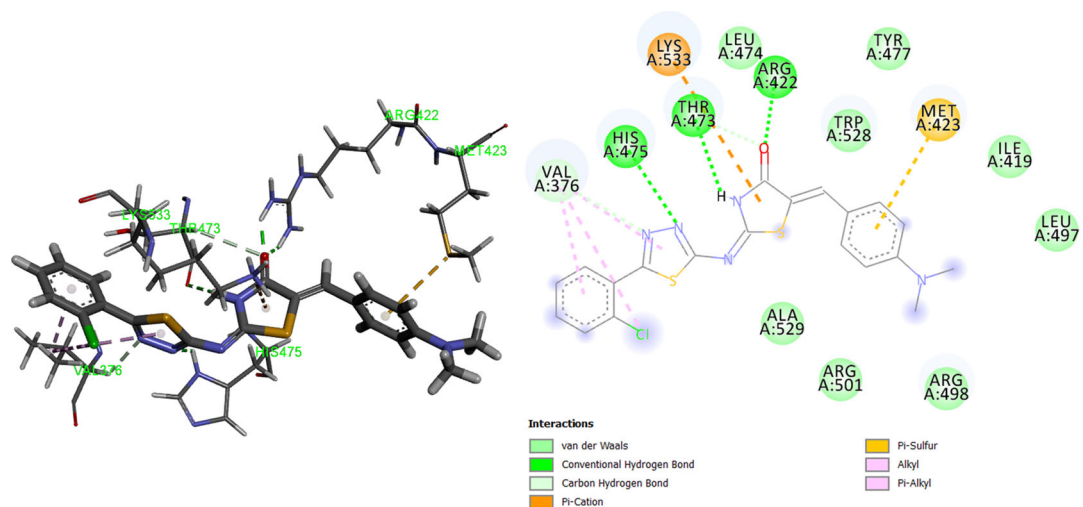


Fig. 10 The 3D (left) and 2D (right) of the docking interactions of compound **7n** with HCV NS5B GT4a thumb II site

Table 2 Analysis of binding interactions of **7b**, **7c**, **7k**, and **7n** with HCV NS5B GT4a thumb II site

Compound	IC ₅₀ (μM)	Hydrogen bonding interactions (distance Å)	Hydrophobic interaction	Pi-cation interaction
7b	0.338	Lys533 (2.32), Thr473 (2.12)	Ile419, Leu482, Leu497, Leu474, Val376, Leu536, Leu469, Gly476, Thr477	Lys533
7c	0.634	His475 (2.21)	Ile419, Leu497, Leu474, Val376, Lys533, Trp528	Lys533
7k	0.564	His475 (2.08), Thr473 (2.58), Arg422 (1.70)	Leu474, Ile419, Val376, Trp528	Lys533
7n	0.342	His475 (2.24), Thr473 (2.61), Arg422 (2.41)	Leu474, Leu497, Ile419, Val376, Lys533, Trp528, Ala529	Lys533

Also, compound **7n** forms three hydrogen bonds with His475, Arg422, Thr473 amino acids, and this can explain its high activity. **7n** shows hydrophobic interactions through aromatic rings with hydrophobic amino acids (Fig. 10 and Table 2).

Antiviral activity on HCV GT4a

Compounds **7a–d**, **7k**, **7n**, **7q**, and **7r** showed the most potent activities with IC₅₀ < 2 μM. Thus, they have been selected for antiviral activity testing. The results illustrated

Table 3 HCV NS5B GT4a antiviral assay of the selected compounds

Compound	Titer (IU/mL)	Fold	% Inhibition
7a	337,790	0.118706	88.13
7b	202,786	0.071263	92.88
7c	148,856	0.052311	94.77
7d	426,019	0.149712	85.03
7k	270,760	0.095151	90.49
7n	578,547	0.203313	79.67
7q	295,742	0.103930	89.61
7r	556,282	0.195489	80.46
Beclabuvir (BMS-791325)	207,376	0.072876	92.72
Positive control	2,845,597	1	0

Table 4 Cytotoxic activity (CC_{50}) of **7a**, **7b**, and **7c** against human hepatoma (Huh7.5) cell line

Compound	$CC_{50}^a \pm SD^b$ (μ M)
7a	58.22 \pm 1.72
7b	176.87 \pm 4.99
7c	133.48 \pm 3.69
Beclabuvir (BMS-791325)	28.05 \pm 0.78

^aThe half-maximal cytotoxic concentration

^bThe standard deviation of triplicate experiments

in Table 3 show that all eight tested compounds exhibited more than 79% inhibition of the HCV GT4a viral activity, which indicates the good activity of these compounds. Compounds **7b** (0.338 μ M, 92.88%) and **7c** (0.634 μ M, 94.77%) have high % inhibition compared to Beclabuvir reference compound (92.72%). Compound **7c** exhibited the highest % inhibition among the tested compounds, while **7b** showed higher IC_{50} with good percentage of inhibition too.

Cytotoxicity study on human hepatoma (Huh7.5) cell line

Compounds **7b** and **7c**, the most active inhibitors, and the lead compound **7a** were subjected to cytotoxicity study on Huh7.5 cell line along with Beclabuvir as a reference compound (Table 4). The assay was carried out using MTT assay kit, in which the detection of cell metabolic activity is based on the purple color that results from biochemical reaction. The developed color is directly proportional to the cell number, which indicates the cell viability.

The results show that all tested compounds exhibited low cytotoxicity on Huh7.5 cell lines compared to Beclabuvir reference compound. Moreover, compound **7b** exhibited the least cytotoxicity by more than six folds compared to Beclabuvir.

Conclusion

Our efforts are directed to develop potent inhibitors of HCV NS5B GT4a for treating HCV GT4a infection. A set of compounds with 4-thiazolidinone derivatives has been designed. To validate the binding affinity of this set of compounds, homology model of HCV NS5B GT4a was constructed and the compounds were docked. Based on the docking results, 18 compounds (**7a–r**) were selected for synthesis and were further evaluated for their activity. Compounds (**7a–r**) were subjected to in vitro HCV NS5B GT4a inhibition assay. Compounds **7b** and **7n** showed the highest inhibitory activity (IC_{50} = 0.338 and 0.342 μ M, respectively). Compounds **7a**, **7b**, **7c**, **7d**, **7k**, **7n**, **7q**, and **7r** with IC_{50} < 2 μ M were selected for the assessment of the anti-HCV GT4a activity using human hepatoma cell line (Huh 7.5), the percentage of inhibition of the tested compounds was between 79.67 and 94.77%. Compounds **7a**, **7b**, and **7c** were tested for their cytotoxicity on the Huh7.5 cell line and exhibited low cytotoxicity compared to Beclabuvir reference compound. Compound **7b** was identified through this study as a potential new lead for future HCV inhibition studies.

Materials and methods

Chemistry

General

Chemical reagents and materials were supplied by Sigma-Aldrich and Alfa Aesar companies and were used without further purification. Electrothermal melting point device (Stuart SMP30) was used for melting points detection, and the results were reported uncorrected. TLC aluminum sheets Silica 60 F₂₅₄ (Merck Co.) were used for reactions monitoring and were visualized with UV light at 254 nm, using TLC system: chloroform/methanol/acetic acid (9.3:0.5:0.2 v/v/v). The PerkinElmer 2400 series II CHNS elemental analyzer was used for elemental analysis. IR spectra of all compounds were recorded on a PerkinElmer FT-IR spectrophotometer using KBr discs with a frequency range of (4000–400 cm^{-1}). ¹H NMR spectra were processed on Bruker FT-NMR (400 MHz) spectrometer using dimethyl sulfoxide (DMSO) as a solvent, and the chemical shifts were reported as ppm. ¹³C NMR spectra of the representative examples (**7b–f**, **7n**, **7q**) were recorded on Bruker FT-NMR (100 MHz) using DMSO-*d*₆ as a solvent with tetramethylsilane as an internal standard. Pyridine was used to dissolve compounds **7b**, **7n**, and **7f** duo to their poor solubility in DMSO. All chemical shift values and multiplicity were quoted in ppm.

General synthetic procedure of 2-(arylmethylidene)hydrazinecarbothioamides (3a–e) [23]

Solutions of thiosemicarbazide **2** (30 mmol) were added to solutions of aldehydes (**1a–e**) (30 mmol), and five drops of acetic acid were added then the reaction mixtures were heated under reflux for 12 h. The products (**3a–e**) were filtered, and the recrystallization was performed using ethanol.

Compounds **3a**, **3d**, and **3e** [23] and compounds **3b** and **3c** [34] were reported.

General synthetic procedure of 5-(substituted phenyl)-1,3,4-thiadiazol-2-amines (4a–e) [23, 24]

Solutions of compounds **3a–e** (2 mmol) in ethanol were added to solutions of ferric chloride (8 mmol). Then the reactions were heated under reflux for 20 h. The reactions were neutralized by ammonia solution, filtered, dried, and the recrystallization was performed using ethanol.

Compounds **4a**, **4d**, and **4e** [23] and compounds **4b** and **4c** [24] were reported.

General synthetic procedure of 2-chloro-N-[5-(substituted phenyl)-1,3,4-thiadiazol-2-yl]acetamides (5a–e) [23, 24]

Compounds **4a–e** (10 mmol) were dissolved in dichloromethane, and triethylamine (12 mmol) was added to the reaction pots. Chloroacetyl chloride (20 mmol) was added to the reaction pots slowly under anhydrous condition, followed by stirring for 4 h under reflux. The reactions were filtered then dried, and the recrystallization was performed using ethanol.

Compounds **5a**, **5d**, and **5e** [23] and compounds **5b** and **5c** [24] were reported.

General synthetic procedure of 2-[[5-(substituted phenyl)-1,3,4-thiadiazol-2-yl]imino]-1,3-thiazolidin-4-ones (6a–e) [23, 24]

Solutions of compounds **5a–e** (2.5 mmol) in 1,4-dioxane were added to ethanolic solutions of ammonium thiocyanate (5 mmol). The reactions were stirred under reflux for 20 h. The solvent was evaporated. The reactions were filtered then dried, and the recrystallization was performed using ethanol.

Compounds **6a**, **6d**, and **6e** [23] and compounds **6b** and **6c** [24] were reported.

General synthetic procedure of 5-(substituted arylidene)-2-[[5-(substituted phenyl)-1,3,4-thiadiazol-2-yl]imino]-1,3-thiazolidin-4-ones (7a–r) [23, 24]

Compounds **6a–e** (1.5 mmol) were dissolved in methanol, then sodium methoxide (3 mmol) in methanol was added, and the mixture was heated for 10 min. The aldehyde

(1.8 mmol) was dissolved in methanol in excess amount and added to the mixture. The reaction mixtures were heated under reflux for 12 h. The reactions were left to cool at 25 °C. Then 40 mL ice-cold water was added. Then the mixtures were neutralized with glacial acetic acid to give compounds **7a–r**. The precipitated products were filtered, washed with water, and the recrystallization was performed using Dimethylformamide.

5-(3-Fluorobenzylidene)-2-[[5-(2-chloro-6-fluorophenyl)-1,3,4-thiadiazol-2-yl]imino]-1,3-thiazolidin-4-one (7a) The results of the characterization of the compound **7a** (shown in Page 2, Supplementary Material) were as reported [23].

5-(1,3-Benzodioxol-5-ylmethylidene)-2-[[5-(2-chloro-6-fluorophenyl)-1,3,4-thiadiazol-2-yl]imino]-1,3-thiazolidin-4-one (7b) Pale yellow solid; yield (0.065 g, 20.2%) with mp 285–289 °C. IR (KBr, cm^{-1}): 3449 (N-H str.), 3145 (Ar-H), 2902 (C-H str. of CH_2), 1705 (C=O, lactam), 1593 (C=N str.). ^1H NMR (400 MHz, $\text{DMSO}-d_6$) δ (ppm): 6.17 (s, 2H, CH_2), 7.17–7.19 (d, 1H, Ar-H21), 7.2 (s, 1H, Ar-H25), 7.27–7.29 (d, 1H, Ar-H22), 7.49–7.53 (t, 1H, Ar-H17), 7.59–7.61 (d, 1H, Ar-H19), 7.67–7.71 (q, 1H, Ar-H18), 7.78 (s, 1H, =CH13), 13.04 (broad s, 1H, NH of lactam). ^{13}C NMR (100 MHz, pyridine) δ (ppm): 102.28 (C27), 109.16 (C21), 109.71 (C22), 114.85 (C6), 115.07 (C17), 122.78 (C15), 123.81 (C20), 126.18 (C25), 126.21 (C19), 132.67 (C23), 132.79 (C24), 134.83 (C13), 135.86 (C18), 148.74 (C16), 149.08 (C10), 150.15 (C2), 159.70 (C8), 162.21 (C4), 198.20 (C11). Anal. Calcd. for $\text{C}_{19}\text{H}_{10}\text{ClFN}_4\text{O}_3\text{S}_2$: C, 49.51; H, 02.19; N, 12.16; S, 13.91%; Found: C, 49.80; H, 02.42; N, 12.35; S, 14.15%.

5-(4-Dimethylaminobenzylidene)-2-[[5-(2-chloro-6-fluorophenyl)-1,3,4-thiadiazol-2-yl]imino]-1,3-thiazolidin-4-one (7c) Orang solid; yield (0.132 g, 38.27 %) with mp 270–273 °C. IR (KBr, cm^{-1}): 3439 (N-H str.), 3142 (Ar-H), 2926 (C-H str. of CH_3), 1699 (C=O, lactam), 1583 (C=N str.). ^1H NMR (400 MHz, $\text{DMSO}-d_6$) δ (ppm): 3.04 (s, 6H, 2- CH_3), 6.89–6.91 (d, 2H, Ar-H), 7.48–7.72 (m, 6H, Ar-H, =CH), 12.84 (s, 1H, NH of lactam). ^{13}C NMR (100 MHz, DMSO) δ (ppm): 40.04 (2 CH_3), 112.66, 115.68, 115.89, 116.27, 120.29, 126.77, 133.05, 134.37 (Ar-C), 135.05 (thiazolidinone C5), 152.14 (=CH-Ar), 160.51, 161.90 (thiadiazole C5, thiazolidinone C2), 154.40 (thiadiazole C2), 167.75 (thiazolidinone C4). Anal. Calcd. for $\text{C}_{20}\text{H}_{15}\text{ClFN}_5\text{OS}_2$: C, 52.23; H, 03.29; N, 15.23; S, 13.94%; Found: C, 52.51; H, 03.49; N, 15.45; S, 13.76%.

5-(3-Chlorobenzylidene)-2-[[5-(2-chloro-6-fluorophenyl)-1,3,4-thiadiazol-2-yl]imino]-1,3-thiazolidin-4-one (7d) Yellow solid; yield (0.443 g, 65.44%) with mp 284–287 °C. IR (KBr, cm^{-1}): 3437 (N-H str.), 3095 (Ar-H), 1714 (C=O, str.),

1598 (C=N str.). ^1H NMR (400 MHz, DMSO- d_6) δ (ppm): 7.48–7.84 (m, 7H, Ar-H), 7.79 (s, 1H, =CH), 13.17 (s, 1H, NH of lactam). ^{13}C NMR (100 MHz, DMSO) δ (ppm): 115.68, 115.89, 126.23, 126.73, 128.42, 130.66, 131.77, 132.06, 134.02, 134.31, 134.34, 134.46, 135.76, 155.18 (Ar-C, =CH-Ar, thiazolidinone C5), 159.39, 159.69 (thiadiazole C5, thiazolidinone C2), 161.89 (thiadiazole C2), 167.33 (thiazolidinone C4). Anal. Calcd. for $\text{C}_{18}\text{H}_9\text{Cl}_2\text{FN}_4\text{OS}_2$: C, 47.90; H, 02.01; N, 12.42; S, 14.21%; Found: C, 47.73; H, 01.83; N, 12.71; S, 13.97%.

5-(3-Phenylpropylidene)-2-[[5-(4-fluorophenyl)-1,3,4-thiadiazol-2-yl]imino]-1,3-thiazolidin-4-one (7e) Yellow solid; yield (0.063 g, 20.46%) with mp 224–226 °C. IR (KBr, cm^{-1}): 3447 (N-H str.), 3084 (Ar-H), 2923 (C-H str. of CH_2), 1728 (C=O, str.), 1585 (C=N str.). ^1H NMR (400 MHz, DMSO- d_6) δ (ppm): 2.61–2.62 (m, 2H, $\text{CH}_2\text{CH}_2\text{-Ph}$), 2.84–2.89 (m, 2H, $\text{CH}_2\text{CH}_2\text{-Ph}$), 6.92–6.94 (t, 1H, =CH), 7.20–7.42 (m, 7H, ArH), 7.97–7.99 (t, 2H, ArH), 12.78 (s, 1H, NH of lactam). ^{13}C NMR (100 MHz, DMSO) δ (ppm): 33.09, 33.59 (2 CH_2) 116.89, 117.11, 126.68, 127.06, 127.83, 128.83, 129.93, 138.09, 140.85 (Ar-C), 159.32 (thiazolidinone C5), 162.82 (=CH-Ar), 164.14, 165.30 (thiadiazole C5, thiazolidinone C2), 166.09 (thiadiazole C2), 170.32 (thiazolidinone C4). Anal. Calcd. for $\text{C}_{20}\text{H}_{15}\text{FN}_4\text{OS}_2$: C, 58.52; H, 03.68; N, 13.65; S, 15.62%; Found: C, 58.78; H, 03.38; N, 13.89; S, 15.37%.

5-(3,4-Dimethoxybenzylidene)-2-[[5-(4-fluorophenyl)-1,3,4-thiadiazol-2-yl]imino]-1,3-thiazolidin-4-one (7f) Yellow solid; yield (0.170 g, 38.49%) with mp 266–268 °C. IR (KBr, cm^{-1}): 3452 (N-H str.), 1640 (C=O st., lactam) 1587 (C=N str.). ^1H NMR (400 MHz, DMSO- d_6) δ (ppm): 3.84 (s, 6H, CH_3), 7.22–8.02 (m, 7H, Ar-H), 8.02 (s, 1H, =CH), 12.92 (s, 1H, NH of lactam); ^{13}C NMR (100 MHz, Pyridine) δ (ppm): 55.66 (2 OCH_3), 112.17, 114.23, 116.26, 116.48, 123.83, 127.60, 129.53, 129.61, 134.84 (Ar-C, =CH-Ar), 135.61 (thiazolidinone C5), 151.52 (thiazolidinone C2), 162.30 (thiazolidinone C4). Anal. Calcd. for $\text{C}_{20}\text{H}_{15}\text{FN}_4\text{O}_3\text{S}_2$: C, 54.29; H, 03.42; N, 12.66; S, 14.49%; Found: C, 54.51; H, 03.62; N, 12.99; S, 14.98%.

5-[[4-(Benzyloxy)-3-methoxyphenyl]methylidene]-2-[[5-(4-chlorophenyl)-1,3,4-thiadiazol-2-yl]imino]-1,3-thiazolidin-4-one (7g) Yellow solid; yield (0.085 g, 23.72%) with mp 259–261 °C. IR (KBr, cm^{-1}): 3451 (N-H str.), 1641 (C=O st., lactam), 1587 (C=N str.). ^1H NMR (400 MHz, DMSO- d_6) δ (ppm): 3.85 (s, 3H, CH_3), 5.19 (s, 2H, CH_2), 7.23–7.78 (m, 12H, Ar-H), 7.97 (d, 1H, =CH), 12.96 (s, 1H, NH of lactam). Anal. Calcd. for $\text{C}_{26}\text{H}_{19}\text{ClN}_4\text{O}_3\text{S}_2$: C, 58.37; H, 03.58; N, 10.47; S, 11.99%; Found: C, 58.56; H, 03.79; N, 10.62; S, 12.26%.

5-(3-Bromobenzylidene)-2-[[5-(3-fluorophenyl)-1,3,4-thiadiazol-2-yl]imino]-1,3-thiazolidin-4-one (7h) Yellow solid; yield (0.075 g, 21.74%) with mp 274–276 °C. IR (KBr, cm^{-1}): 1721 (C=O st., lactam), 1610 (C=N str.). ^1H NMR (400 MHz, DMSO- d_6) δ (ppm): 7.40–7.80 (m, 8H, Ar-H), 7.90 (s, 1H, =CH), 13.12 (s, 1H, NH of lactam). Anal. Calcd. for $\text{C}_{18}\text{H}_{10}\text{BrFN}_4\text{OS}_2$: C, 46.86; H, 02.19; N, 12.15; S, 13.89%; Found: C, 46.99; H, 01.92; N, 11.98; S, 14.21%.

5-(2-Bromobenzylidene)-2-[[5-(3-fluorophenyl)-1,3,4-thiadiazol-2-yl]imino]-1,3-thiazolidin-4-one (7i) Yellow solid; yield (0.058 g, 16.76%) with mp 267–268 °C. IR (KBr, cm^{-1}): 3434 (N-H str.), 1724 (C=O st., lactam), 1603 (C=N str.). ^1H NMR (400 MHz, DMSO- d_6) δ (ppm): 7.41–7.85 (m, 8H, Ar-H), 7.90 (s, 1H, =CH), 13.18 (s, 1H, NH of lactam). Anal. Calcd. for $\text{C}_{18}\text{H}_{20}\text{BrNO}_4$: C, 46.86; H, 02.19; N, 12.15; S, 13.89%; Found: C, 46.57; H, 02.48; N, 12.42; S, 13.61%.

5-(4-Dimethylaminobenzylidene)-2-[[5-(3-fluorophenyl)-1,3,4-thiadiazol-2-yl]imino]-1,3-thiazolidin-4-one (7j) Orange solid; yield (0.093 g, 29.14%) with mp 255–258 °C. IR (KBr, cm^{-1}): 3448 (N-H str.), 3145 (Ar-H), 1699 (C=O st., lactam), 1583 (C=N str.). ^1H NMR (400 MHz, DMSO- d_6) δ (ppm): 3.06 (s, 6H, 2 CH_3), 7.71 (s, 1H, =CH), 6.90–7.82 (8H, Ar-H), 12.81 (s, 1H, NH of lactam). Anal. Calcd. for $\text{C}_{20}\text{H}_{16}\text{FN}_5\text{OS}_2$: C, 56.45; H, 03.79; N, 16.46; S, 15.07%; Found: C, 56.68; H, 04.10; N, 16.71; S, 15.32%.

5-(3-Chlorobenzylidene)-2-[[5-(3-fluorophenyl)-1,3,4-thiadiazol-2-yl]imino]-1,3-thiazolidin-4-one (7k) Yellow solid; yield (0.158 g, 50.54%) with mp 275–278 °C. IR (KBr, cm^{-1}): 3448 (N-H str.), 3151 (Ar-H), 1709 (C=O str., lactam), 1593 (C=N str.). ^1H NMR (400 MHz, DMSO- d_6) δ (ppm): 7.41–7.95 (m, 9H, ArH, =CH), 13.13 (s, 1H, NH of lactam). Anal. Calcd. for $\text{C}_{18}\text{H}_{10}\text{ClFN}_4\text{OS}_2$: C, 51.86; H, 02.42; N, 13.44; S, 15.38%; Found: C, 51.56; H, 02.14; N, 13.14; S, 15.11%.

5-(4-Methoxybenzylidene)-2-[[5-(3-fluorophenyl)-1,3,4-thiadiazol-2-yl]imino]-1,3-thiazolidin-4-one (7l) Yellow solid; yield (0.050 g, 24.25%) with mp 267–270 °C. IR (KBr, cm^{-1}): 3448 (N-H str.), 3100 (Ar-H), 1702 (C=O st., lactam), 1587 (C=N str.). ^1H NMR (400 MHz, DMSO- d_6) δ (ppm): 3.84 (s, 3H, CH_3), 7.16–7.80 (m, 9H, Ar-H, =CH), 12.96 (s, 1H, NH of lactam). Anal. Calcd. for $\text{C}_{18}\text{H}_{13}\text{FN}_4\text{O}_2\text{S}_2$: C, 55.33; H, 03.18; N, 13.59; S, 15.55%; Found: C, 55.02; H, 02.95; N, 13.83; S, 15.23%.

5-[[4-(Benzyloxy)-3-methoxyphenyl]methylidene]-2-[[5-(2-chlorophenyl)-1,3,4-thiadiazol-2-yl]imino]-1,3-thiazolidin-4-one (7m) Yellow solid; yield (0.420 g, 52.33%) with mp 250–252 °C. IR (KBr, cm^{-1}): 3450 (N-H str.), 1688 (C=O

st., lactam), 1577 (C=N str.). ^1H NMR (400 MHz, DMSO- d_6) δ (ppm): 3.85 (s, 3H, CH₃), 5.19 (s, 2H, CH₂), 7.26–8.20 (m, 12H, Ar-H), 8.2 (d, 1H, =CH), 12.98 (s, 1H, NH of lactam). Anal. Calcd. for C₂₆H₁₉ClN₄O₃S₂: C, 58.37; H, 03.58; N, 10.47; S, 11.99%; Found: C, 58.68; H, 03.77; N, 10.19; S, 12.28%.

5-(4-Dimethylaminobenzylidene)-2-[[5-(2-chlorophenyl)-1,3,4-thiadiazol-2-yl]imino]-1,3-thiazolidin-4-one (7n)

Orange solid; yield (0.076 g, 22.98%) with mp 291–294 °C. IR (KBr, cm⁻¹): 3450 (N-H str.), 1697 (C=O st., lactam), 1577 (C=N str.). ^1H NMR (400 MHz, DMSO- d_6) δ (ppm): 3.04 (s, 6H, 2 CH₃), 8.10 (d, 1H, =CH), 6.89–7.73 (8H, Ar-H), 12.82 (s, 1H, NH of lactam). ^{13}C NMR (100 MHz, Pyridine) δ (ppm): 33.17 (2 CH₃), 106.02, 114.73, 116.54, 117.58, 121.37, 123.7, 124.55, 125.32, 125.92(Ar-C), 145.4 (thiazolidinone C5), 126.52 (=CH-Ar), 129.6, 129.35 (thiadiazole C5, thiazolidinone C2), 128.28 (thiadiazole C2), 153.91 (thiazolidinone C4). Anal. Calcd. for C₂₀H₁₆ClN₅O₂S₂: C, 54.35; H, 03.65; N, 15.85; S, 14.51%; Found: C, 54.59; H, 03.87; N, 16.10; S, 14.81%.

5-(3-Bromobenzylidene)-2-[[5-(2-chlorophenyl)-1,3,4-thiadiazol-2-yl]imino]-1,3-thiazolidin-4-one (7o) Yellow solid; yield (0.108 g, 30.14%) with mp 280–283 °C. IR (KBr, cm⁻¹): 3449 (N-H str.), 1704 (C=O st., lactam), 1594 (C=N str.). ^1H NMR (400 MHz, DMSO- d_6) δ (ppm): 7.57–7.91 (m, 8H, Ar-H), 8.20 (d, 1H, =CH), 13.15 (s, 1H, NH of lactam); Anal. Calcd. for C₁₈H₁₀BrClN₄O₂S₂: C, 45.25; H, 2.11; N, 11.73; S, 13.42%; Found: C, 45.51; H, 1.84; N, 11.44; S, 13.17%.

5-(3-Chlorobenzylidene)-2-[[5-(2-chlorophenyl)-1,3,4-thiadiazol-2-yl]imino]-1,3-thiazolidin-4-one (7p) Yellow solid; yield (0.107 g, 32.92%) with mp 270–271 °C. IR (KBr, cm⁻¹): 3449 (N-H str.), 1709 (C=O st., lactam), 1592 (C=N str.). ^1H NMR (400 MHz, DMSO- d_6) δ (ppm): 7.57–7.81 (m, 8H, Ar-H), 8.20 (d, 1H, =CH), 13.14 (s, 1H, NH of lactam). Anal. Calcd. for C₁₈H₁₀Cl₂N₄O₂S₂: C, 49.89; H, 02.33; N, 12.93; S, 14.79%; Found: C, 50.21; H, 2.11; N, 12.75%; S, 15.10%.

5-(3-Nitrobenzylidene)-2-[[5-(2-chlorophenyl)-1,3,4-thiadiazol-2-yl]imino]-1,3-thiazolidin-4-one (7q) Yellow solid; yield (0.165 g, 49.56%) with mp 272–274 °C. IR (KBr, cm⁻¹): 3419 (N-H str.), 3121 (Ar-H), 1726 (C=O st., lactam), 1596 (C=N str.). ^1H NMR (400 MHz, DMSO- d_6) δ (ppm): 7.54–8.32 (m, 8H, Ar-H), 8.52 (s, 1H, =CH), 13.19 (s, 1H, NH of lactam). ^{13}C NMR (100 MHz, DMSO) δ (ppm): 125.04, 125.15, 127.44, 128.47, 128.98, 131.05, 131.19, 131.46, 131.71, 132.79, 135.26, 136.00, (Ar-C), 148.73 (thiazolidinone C5), 160.72 (=CH-Ar), 158.87 (thiadiazole C5), 158.80 (thiazolidinone C2),

167.18 (thiadiazole C2), 171.36 (thiazolidinone C4). Anal. Calcd. for C₁₈H₁₀ClN₅O₃S₂: C, 48.70; H, 02.28; N, 15.78; S, 14.45%; Found: C, 49.01; H, 02.56; N, 15.49; S, 14.72%.

5-(4-Methoxybenzylidene)-2-[[5-(2-chlorophenyl)-1,3,4-thiadiazol-2-yl]imino]-1,3-thiazolidin-4-one (7r) Yellow solid; yield (0.133 g, 41.36%) with mp 279–281 °C. IR (KBr, cm⁻¹): 3422 (N-H str.), 3097 (Ar-H), 1701 (C=O st., lactam), 1587 (C=N str.). ^1H NMR (400 MHz, DMSO- d_6) δ (ppm): 3.84 (s, 3H, CH₃), 7.17–7.78 (m, 8H, Ar-H), 8.10 (d, 1H, =CH), 12.98 (s, 1H, NH of lactam). Anal. Calcd. for C₁₉H₁₃ClN₄O₂S₂: C, 53.21; H, 03.06; N, 13.07; S, 14.95%; Found: C, 53.52; H, 02.85; N, 13.32; S, 15.23%.

Biology

In vitro HCV NS5B inhibition assay

Scintillation proximity assay (SPA) was used to evaluate the HCV NS5B inhibition using SPA beads. The beads emit an amount of light that is detected using a top count plate reader (Packard Top Count NXT scintillation counter, PerkinElmer). The detailed assay protocol was carried out as described (Page 31 and Supplementary Fig. S61–S78, Supplementary Material), and as reported [35, 36].

Antiviral activity

Huh-7.5 cells (ATCC code PTA-8561) were cultured as reported [36], the detailed procedure was carried out as described (Page 40, Supplementary Material). The infected Huh-7.5 cells were cultured and then serial concentrations of the tested compounds were added after incubation. The level of HCV RNA in each sample was assessed by quantitative real-time PCR on Rotor-Gene Cycler (Qiagen). The test was carried out using a commercially available kit supplied by “DNA-Technology, Research & Production” LLC (Moscow, Russia) according to the manufacturer’s instructions. The primers used for HCV and GAPDH internal control were previously reported [37]. The percent inhibition was calculated for each sample (Supplementary Fig. S79, Supplementary Material) as previously described [36].

Cytotoxicity study

Huh-7.5 cells were cultured, and cytotoxicity of the tested compounds was measured using MTT kit (Sigma-Aldrich) as described by the manufacturer. The detailed procedure was carried out as described (Page 42, Supplementary Fig. S80–S83, Supplementary Material) [35].

Computational studies

Homology modeling

The sequence for HCV NS5B domain, which consists of 591 amino acids, was retrieved from the UniProtKB database [25] with feature key: (ChainiPRO_0000045543) and entry number (O39929) for HCV GT4a. The sequence was used to build a model using SWISS-MODEL [27] online server. The FASTA sequence was used to identify the templates with high identity using BLAST server [38], then selection of the highest identity template with reliable coverage and GMQE to be used in the second step, which is model building. After the model was built, the model is subjected to protein refinement using the ModRefiner server [26].

Molecular docking

A set of compounds was sketched using MarvinSketch 5.11.5 [39]. OMEGA-3.1.0.3 [40] was used to generate 3D conformations of compounds using torsion driving and distance geometry algorithms. The output library file of OMEGA-3.1.0.3 [40] was ready for docking using OEDocking 3.3.0.3 [41] software against the HCV NS5B GT4a homology model with box dimensions 33.67 Å × 35.00 Å × 25.33 Å, the software set to generate five poses for each compound.

Discovery Studio 2019 Client software [42] was used for 2D and 3D visualization of the docking poses and the interactions between the target and the docked compounds. HCV NS5B protein binding site is shown in wireframe presentation. The atoms color scheme is that gray represents carbon, white represents hydrogen, blue represents nitrogen, red represents oxygen, yellow represents sulfur, and H bonds are represented as dotted green lines.

Acknowledgements We are grateful for OpenEye Scientific Software for supporting the academic license granted to MAE laboratory. We also thank Dr. Khaled M. Elokely, Tanta University, for his help in analyzing the computational data and Dr. Ahmed E. Goda, Tanta University, for his help in the biological studies.

Author contributions MAE contributed to conceptualization and design. ASA-B collected the data and carried out the experimental section. All authors analyzed the data, wrote, and revised the manuscript.

Compliance with ethical standards

Conflict of interest The authors declare no competing interests.

Publisher's note Springer Nature remains neutral with regard to jurisdictional claims in published maps and institutional affiliations.

References

1. WHO. Hepatitis C fact sheet. 2019. <https://www.who.int/news-room/fact-sheets/detail/hepatitis-c>. Accessed July 29 2020.
2. Jafri SM, Gordon SC. Epidemiology of hepatitis C. *Clin Liver Dis.* 2018;12:140–2. <https://doi.org/10.1002/cld.783>
3. Alexopoulou A, Karayiannis P. Interferon-based combination treatment for chronic hepatitis C in the era of direct acting antivirals. *Ann Gastroenterol.* 2015;28:55–65.
4. Smith K. Sofosbuvir: a new milestone in HCV treatment? *Nat Rev Gastroenterol Hepatol.* 2013;10:258– <https://doi.org/10.1038/nrgastro.2013.60>
5. Götte M, Feld JJ. Direct-acting antiviral agents for hepatitis C: structural and mechanistic insights. *Nat Rev Gastroenterol Hepatol.* 2016;13:338–51. <https://doi.org/10.1038/nrgastro.2016.60>
6. Legrand-Abravanel F, Henquell C, Le Guillou-Guillemette H, Balan V, Mirand A, Dubois M, et al. Naturally occurring substitutions conferring resistance to hepatitis C virus polymerase inhibitors in treatment-naïve patients infected with genotypes 1-5. *Antivir Ther.* 2009;14:723–30.
7. El-Tahan RR, Ghoneim AM, Zaghoul H. Dissection of two drug-targeted regions of Hepatitis C virus subtype 4a infecting Egyptian patients. *Virus Genes.* 2020. <https://doi.org/10.1007/s11262-020-01776-y>.
8. Bartenschlager R, Lohmann V, Penin F. The molecular and structural basis of advanced antiviral therapy for hepatitis C virus infection. *Nat Rev Microbiol.* 2013;11:482–96. <https://doi.org/10.1038/nrmicro3046>
9. Di Maio VC, Cento V, Mirabelli C, Artese A, Costa G, Alcaro S, et al. Hepatitis C virus genetic variability and the presence of NS5B resistance-associated mutations as natural polymorphisms in selected genotypes could affect the response to NS5B inhibitors. *Antimicrob Agents Chemother.* 2014;58:2781–97. <https://doi.org/10.1128/aac.02386-13>
10. Watkins WJ. Evolution of HCV NS5B non-nucleoside inhibitors. In: Sofia M, editor. *HCV: the journey from discovery to a cure.* Cham: Springer; 2019. p. 171–91.
11. Li H, Tatlock J, Linton A, Gonzalez J, Borchardt A, Dragovich P, et al. Identification and structure-based optimization of novel dihydropyrones as potent HCV RNA polymerase inhibitors. *Bioorg Med Chem Lett.* 2006;16:4834–8. <https://doi.org/10.1016/j.bmcl.2006.06.065>
12. Li P, Dorsch W, Lauffer DJ, Bilimoria D, Chauret N, Court JJ, et al. Discovery of novel allosteric HCV NS5B inhibitors. 2. lactam-containing thiophene carboxylates. *ACS Med Chem Lett.* 2017;8:251–5. <https://doi.org/10.1021/acsmchemlett.6b00479>
13. Yan S, Appleby T, Larson G, Wu JZ, Hamatake R, Hong Z, et al. Structure-based design of a novel thiazolone scaffold as HCV NS5B polymerase allosteric inhibitors. *Bioorg Med Chem Lett.* 2006;16:5888–91. <https://doi.org/10.1016/j.bmcl.2006.08.056>
14. Li H, Tatlock J, Linton A, Gonzalez J, Jewell T, Patel L, et al. Discovery of (R)-6-cyclopentyl-6-(2-(2,6-diethylpyridin-4-yl)ethyl)-3-((5,7-dimethyl-[1,2,4]triazolo[1,5-a]pyrimidin-2-yl)methyl)-4-hydroxy-5,6-dihydropyran-2-one (PF-00868554) as a potent and orally available hepatitis C virus polymerase inhibitor. *J Med Chem.* 2009;52:1255–8. <https://doi.org/10.1021/jm8014537>
15. Lazerwith SE, Lew W, Zhang J, Morganello P, Liu Q, Canales E, et al. Discovery of GS-9669, a thumb site II non-nucleoside inhibitor of NS5B for the treatment of genotype I chronic hepatitis C infection. *J Med Chem.* 2014;57:1893–901. <https://doi.org/10.1021/jm401420j>
16. Shi ST, Herlihy KJ, Graham JP, Nonomiya J, Rahavendran SV, Skor H, et al. Preclinical characterization of PF-00868554, a potent nonnucleoside inhibitor of the hepatitis C virus RNA-

- dependent RNA polymerase. *Antimicrob Agents Chemother.* 2009;53:2544–52. <https://doi.org/10.1128/aac.01599-08>
17. Ding Y, Smith KL, Varaprasad CVNS, Chang E, Alexander J, Yao N. Synthesis of thiazolone-based sulfonamides as inhibitors of HCV NS5B polymerase. *Bioorg Med Chem Lett.* 2007;17:841–5. <https://doi.org/10.1016/j.bmcl.2006.08.104>
 18. Babaoğlu K, Page MA, Jones VC, McNeil MR, Dong C, Naismith JH, et al. Novel inhibitors of an emerging target in *Mycobacterium tuberculosis*; substituted thiazolidinones as inhibitors of dTDP-rhamnose synthesis. *Bioorg Med Chem Lett.* 2003;13:3227–30. [https://doi.org/10.1016/S0960-894X\(03\)00673-5](https://doi.org/10.1016/S0960-894X(03)00673-5)
 19. Küçükgül G, Kocatepe A, De Clercq E, Şahin F, Güllüce M. Synthesis and biological activity of 4-thiazolidinones, thiosemicarbazides derived from difluorhydrazide. *Eur J Med Chem.* 2006;41:353–9. <https://doi.org/10.1016/j.ejmech.2005.11.005>
 20. Ottanà R, Carotti S, Maccari R, Landini I, Chiricosta G, Caciagli B, et al. In vitro antiproliferative activity against human colon cancer cell lines of representative 4-thiazolidinones. Part I. *Bioorg Med Chem Lett.* 2005;15:3930–3. <https://doi.org/10.1016/j.bmcl.2005.05.093>
 21. Kumar A, Rajput CS, Bhati SK. Synthesis of 3-[4'-(p-chlorophenyl)-thiazol-2'-yl]-2-[(substituted azetidione/thiazolidinone)-aminomethyl]-6-bromoquinazolin-4-ones as anti-inflammatory agent. *Bioorg Med Chem.* 2007;15:3089–96. <https://doi.org/10.1016/j.bmc.2007.01.042>
 22. Rawal RK, Tripathi R, Katti SB, Pannecouque C, De Clercq E. Design, synthesis, and evaluation of 2-aryl-3-heteroaryl-1,3-thiazolidin-4-ones as anti-HIV agents. *Bioorg Medicinal Chem.* 2007;15:1725–31. <https://doi.org/10.1016/j.bmc.2006.12.003>
 23. Çakır G, Küçükgül İ, Guhamazumder R, Tatar E, Manvar D, Basu A, et al. Novel 4-thiazolidinones as non-nucleoside inhibitors of hepatitis C virus NS5B RNA-dependent RNA polymerase. *Arch Pharm.* 2015;348:10–22. <https://doi.org/10.1002/ardp.201400247>
 24. Küçükgül İ, Satılmış G, Gurukumar KR, Basu A, Tatar E, Nichols DB, et al. 2-Heteroarylrimino-5-arylidene-4-thiazolidinones as a new class of non-nucleoside inhibitors of HCV NS5B polymerase. *Eur J Med Chem.* 2013;69:931–41. <https://doi.org/10.1016/j.ejmech.2013.08.043>
 25. UniProt Consortium. UniProt: the universal protein knowledge-base. *Nucleic Acids Res.* 2018;46:2699–. <https://doi.org/10.1093/nar/gky092>
 26. Xu D, Zhang Y. Improving the physical realism and structural accuracy of protein models by a two-step atomic-level energy minimization. *Biophys J.* 2011;101:2525–34. <https://doi.org/10.1016/j.bpj.2011.10.024>
 27. Waterhouse A, Bertoni M, Bienert S, Studer G, Tauriello G, Gumienny R, et al. SWISS-MODEL: homology modelling of protein structures and complexes. *Nucleic Acids Res.* 2018;46:W296–W303. <https://doi.org/10.1093/nar/gky427>
 28. Barreca ML, Iraci N, Manfroni G, Cecchetti V. Allosteric inhibition of the hepatitis C virus NS5B polymerase: in silico strategies for drug discovery and development. *Future Med Chem.* 2011;3:1027–55. <https://doi.org/10.4155/fmc.11.53>
 29. Shih M-H, Wu C-L. Efficient syntheses of thiadiazoline and thiadiazole derivatives by the cyclization of 3-aryl-4-formylsulfonamide thiosemicarbazones with acetic anhydride and ferric chloride. *Tetrahedron.* 2005;61:10917–25. <https://doi.org/10.1016/j.tet.2005.08.107>
 30. Vicini P, Geronikaki A, Anastasia K, Incerti M, Zani F. Synthesis and antimicrobial activity of novel 2-thiazolylimino-5-arylidene-4-thiazolidinones. *Bioorg Medicinal Chem.* 2006;14:3859–64. <https://doi.org/10.1016/j.bmc.2006.01.043>
 31. Vicini P, Geronikaki A, Incerti M, Zani F, Dearden J, Hewitt M. 2-Heteroarylrimino-5-benzylidene-4-thiazolidinones analogues of 2-thiazolylimino-5-benzylidene-4-thiazolidinones with antimicrobial activity: synthesis and structure–activity relationship. *Bioorg Med Chem.* 2008;16:3714–24. <https://doi.org/10.1016/j.bmc.2008.02.001>
 32. Behbehani H, Ibrahim HM. 4-Thiazolidinones in heterocyclic synthesis: synthesis of novel enamionones, azolopyrimidines and 2-arylimino-5-arylidene-4-thiazolidinones. *Molecules.* 2012;17:6362–85.
 33. Cousins KR. ChemDraw Ultra 9.0. CambridgeSoft, 100 CambridgePark Drive, Cambridge, MA 02140. www.cambridgesoft.com. See Web site for pricing options. *J Am Chem Soc.* 2005;127:4115–6. <https://doi.org/10.1021/ja0410237>
 34. Tu G, Li S, Huang H, Li G, Xiong F, Mai X, et al. Novel aminopeptidase N inhibitors derived from 1,3,4-thiadiazole scaffold. *Bioorg Med Chem.* 2008;16:6663–8. <https://doi.org/10.1016/j.bmc.2008.05.081>
 35. Sun J-M, Kim S-J, Kim G-W, Rhee J-K, Kim ND, Jung H, et al. Inhibition of hepatitis C virus replication by monascus pigment derivatives that interfere with viral RNA polymerase activity and the mevalonate biosynthesis pathway. *J Antimicrob Chemother.* 2011;67:49–58. <https://doi.org/10.1093/jac/dkr432>
 36. Hassan GS, Georgy HH, Mohammed EZ, Omar FA. Anti-hepatitis-C virus activity and QSAR study of certain thiazolidinone and thiazolotriazine derivatives as potential NS5B polymerase inhibitors. *Eur J Med Chem.* 2019;184:111747–62. <https://doi.org/10.1016/j.ejmech.2019.111747>
 37. Howe AYM, Bloom J, Baldick CJ, Benetatos CA, Cheng H, Christensen JS, et al. Novel nonnucleoside inhibitor of hepatitis C virus RNA-dependent RNA polymerase. *Antimicrob Agents Chemother.* 2004;48:4813–21. <https://doi.org/10.1128/aac.48.12.4813-4821.2004>
 38. Ye J, McGinnis S, Madden TL. BLAST: improvements for better sequence analysis. *Nucleic acids Res.* 2006;34:6–9. <https://doi.org/10.1093/nar/gkl164>
 39. Nero TL, Parker MW, Morton CJ. Protein structure and computational drug discovery. *Biochem Soc Trans.* 2018;46:1367–79. <https://doi.org/10.1042/bst20180202>
 40. Hawkins PCD, Skillman AG, Warren GL, Ellingson BA, Stahl MT. Conformer generation with OMEGA: Algorithm and validation using high quality structures from the protein databank and cambridge structural database. *J Chem Inf Model.* 2010;50:572–84. <https://doi.org/10.1021/ci100031x>
 41. McGann M. FRED and HYBRID docking performance on standardized datasets. *J Comput Aided Mol Des.* 2012;26:897–906. <https://doi.org/10.1007/s10822-012-9584-8>
 42. BIOVIA. Discovery studio Visualizer v19.1.0.18287. San Diego: Dassault Systèmes 2019.
 43. DeLano WL. Pymol: an open-source molecular graphics tool. *CCP4 Newsl Protein Crystallogr.* 2002;40:82–92.